

Alma Mater Studiorum Università di Bologna
Archivio istituzionale della ricerca

Turning Donepezil into a Multi-Target-Directed Ligand through a Merging Strategy

This is the final peer-reviewed author's accepted manuscript (postprint) of the following publication:

Published Version:

Turning Donepezil into a Multi-Target-Directed Ligand through a Merging Strategy / Perone R.; Albertini C.; Uliassi E.; Di Pietri F.; de Sena Murteira Pinheiro P.; Petralla S.; Rizzardi N.; Fato R.; Pulkrabkova L.; Soukup O.; Tramarin A.; Bartolini M.; Bolognesi M.L.. - In: CHEMMEDCHEM. - ISSN 1860-7179. - ELETTRONICO. - 16:1(2021), pp. 187-198. [10.1002/cmdc.202000484]

Availability:

This version is available at: <https://hdl.handle.net/11585/786577> since: 2021-01-04

Published:

DOI: <http://doi.org/10.1002/cmdc.202000484>

Terms of use:

Some rights reserved. The terms and conditions for the reuse of this version of the manuscript are specified in the publishing policy. For all terms of use and more information see the publisher's website.

This item was downloaded from IRIS Università di Bologna (<https://cris.unibo.it/>).
When citing, please refer to the published version.

(Article begins on next page)

This is the final peer-reviewed accepted manuscript of:

Perone, R.C.; Albertini, C.; Uliassi, E.; Di Pietri, F.; de Sena Murteira Pinheiro, P.; Petralla, S.; Rizzardi, N.; Fato, R.; Pulkrábková, L.; Soukup, O.; Tramarin, A.; Bartolini, M.; Bolognesi, M. L. Turning donepezil in a multi-target-directed ligand through a merging strategy, *ChemMedChem* 2021, 16 (3), 187-198.

The final published version is available online at: <https://chemistry-europe.onlinelibrary.wiley.com/doi/10.1002/cmdc.202000484>

Terms of use:

Some rights reserved. The terms and conditions for the reuse of this version of the manuscript are specified in the publishing policy. For all terms of use and more information see the publisher's website.

This item was downloaded from IRIS Università di Bologna (<https://cris.unibo.it/>)

When citing, please refer to the published version.

DOI: 10.1002/cmdc.202000484

Full Paper

Received: 4. July. 2020

Accepted Article published: 27. Juli 2020

Turning Donepezil into a Multi-Target-Directed Ligand through a Merging Strategy

Dr. Rosaria Perone,^[a] Claudia Albertini,^[a] Dr. Elisa Uliassi,^[a] Flaminia Di[^]Pietri,^[a] Pedro de[^]Sena[^]Murteira[^]Pinheiro,^[a,b] Dr. Sabrina Petralla,^[a] Nicola Rizzardi,^[a] Prof. Romana Fato,^[a] Dr. Lenka Pulkrabkova,^[c,d] Dr. Ondrej Soukup,^[c] Dr. Anna Tramarin,^[a] Prof. Manuela Bartolini,^[a] Prof. Maria[^]Laura Bolognesi0000-0002-1289-5361*^[a]

[a] <orgDiv/>Department of Pharmacy and Biotechnology
<orgName/>Alma Mater Studiorum -- University of Bologna
<street/>Via Belmeloro 6/Via Irnerio 48/Via Selmi 3
<postCode/>40126 <city/>Bologna (<country/>Italy)
E-mail: marialaura.bolognesi@unibo.it

[b] <orgDiv/>Programa de Pós-Graduação em Farmacologia e Química Medicinal
<orgDiv/>Instituto de Ciências Biomédicas
<orgName/>Universidade Federal do Rio de Janeiro
<postCode/>21941-902, <city/>Rio de Janeiro, RJ (<country/>Brazil)

[c] <orgDiv/>Biomedical Research Center
<orgName/>University Hospital Hradec Kralove
<street/>Sokolska 581, <postCode/>500 05, <city/>Hradec Kralove (<country/>Czech Republic)

[d] <orgDiv/>Department of Toxicology and Military Pharmacy
<orgDiv/>Faculty of Military Health Sciences
<orgName/>University of Defence, <city/>Trebesska <postCode/>1575

<pict> Supporting information for this article is available on the WWW under
<url><http://dx.doi.org/10.1002/cmdc.202000484></url>

<spi> This article belongs to the Special Collection "NMMC 2019: DCF-SCI 40th Anniversary".

Alzheimer's disease
drug design
medicinal chemistry

multi-target drug discovery
polypharmacology

Turning donepezil into a multi-target-directed ligand through a merging strategy (Bolognesi @UniboMagazine)

Strike! Starting from a proposed drug combination of idebenone and donepezil, we rationally designed and synthesized a small library of highly merged donepezil-based multi-target-directed ligands (MTDLs), obtained by indanone bioisosteric substitution. The new MTDL **9** has been shown to hit Alzheimer's disease by cholinesterase inhibition, together with A β and oxidative pathway modulation.

Thanks to the widespread use and safety profile of donepezil (**1**) in the treatment of Alzheimer's disease (AD), one of the most widely adopted multi-target-directed ligand (MTDL) design strategies is to modify its molecular structure by linking a second fragment carrying an additional AD-relevant biological property. Herein, supported by a proposed combination therapy of **1** and the quinone drug idebenone, we rationally designed novel **1**-based MTDLs targeting A β and oxidative pathways. By exploiting a bioisosteric replacement of the indanone core of **1** with a 1,4-naphthoquinone, we ended up with a series of highly merged derivatives, in principle devoid of the "physicochemical challenge" typical of large hybrid-based MTDLs. A preliminary investigation of their multi-target profile identified **9**, which showed a potent and selective butyrylcholinesterase inhibitory activity, together with antioxidant and antiaggregating properties. In addition, it displayed a promising drug-like profile.

Introduction

According to WHO data, dementia currently affects about 10 million people in the European Region, and its prevalence is expected to double by 2030.^[1] Sadly, there is no treatment that can cure Alzheimer's disease (AD) or any other type of dementia.^[2] Even more sadly, no new treatment is on the horizon. Over the last decade, more than 200 drug candidates have successfully completed phase II clinical trials, but none has passed phase III.^[3] Actually, there has been no new AD therapy introduced into the market since 2003.^[4] The drug (GV-971) newly approved in China for the treatment of mild to moderate AD, still needs further clinical trials before entering into EU and American markets.^[4] This gloomy situation is exacerbated by the fact that many pharmaceutical companies have abandoned the sector because of the continued clinical failures. The community of AD patients and their

families, researchers, clinicians and Alzheimer associations worldwide are eagerly looking for the development of effective therapies to treat or delay the onset of this devastating disorder. Thus, it is a social responsibility to stay in the field and pushing ahead by using all the knowledge acquired so far to solve this needle-in-haystack problem.^[5]

Currently, the available AD medicines (donepezil (**1**), rivastigmine (**2**), galantamine (**3**) and memantine (**4**), Figure¹) can only temporarily alleviate symptoms, or slow down their progression, and only in selected patients.^[6] The three cholinesterase (ChE) inhibitors **1--3** are efficacious for mild to moderate AD, but It is not possible to identify those patients who respond, prior to treatment.^[7] Despite slight variations in the mode of action, there is no evidence of any differences among **1--3** with respect to clinical efficacy. However, it seems that less adverse effects are associated with **1**.^[7]

Notwithstanding the moderate clinical efficacy, **1** is still a leading therapeutic in the treatment of AD and a classic in chemical neuroscience.^[8]

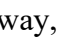
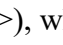
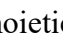
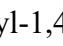
As medicinal chemists working in the field for more than 20⁺years, we are convinced that a rationally designed polypharmacology is the only approach that can confront the complexity of AD pathology and provide a truly disease-modifying therapeutic effect.^[9] On this basis, we envisioned that enriching the **acetylcholinesterase** (AChE) inhibitory effect of **1** with other activities directed to crucial AD targets, could provide derivatives with enhanced clinical potential. This strategy has been extensively followed by us and others in the search of novel multitarget-directed ligands (MTDLs) against AD.^[10]

In particular, we aimed to develop MTDLs whose multitargeted mechanism would not only improve cognitive function via ChE inhibition, but also affect causative processes, such as amyloid beta (A β) cascade and oxidative stress.^[11]

Design

Herein, we manipulated **1**'s structure with the goal of transforming it from a ChE inhibitor into an MTDL for AD. To note, a similar strategy has been pursued for the development of donepezil-ebesen hybrids.^[12]

Structurally, donepezil is composed by a 5,6-dimethoxy-1-indanone core and 1-benzyl-4-piperidine connected by a methylene linker. According to the solved crystal structure,^[13] its binding at human AChE involves several contacts and spans all the enzyme active site gorge. The two aromatic groups at the two ends are critical: the benzyl ring stacks against W86 of the active site, while the indanone ring stacks against W286 of the peripheral anionic site (PAS).

In our effort to preserve the ChE inhibitory activity of **1** and to add anti-amyloid and antioxidant effects, we replaced the indanone scaffold with the bioisosteric 1,4-naphthoquinone (Figure²)². In this way, we sought to combine the anticholinesterase activity with the well-known inhibitory activity of quinones against A β assembly and oxidative stress. In fact, we had successfully reported the development of tacrine-naphthoquinones hybrids (Figure²)², which effectively counteracted amyloid aggregation and ROS production at a cellular level.^[14] In recent years, the diverse set of pharmacological activities displayed makes 1,4-naphthoquinone a very attractive building block for the development of novel drugs. In fact, several studies have shown that it can exhibit neuroprotective effects^[15] and disrupt A β aggregation.^[16] This reinforces the idea that naphthoquinone derivatives may play a key role in AD drug discovery. Based on our previous findings,^[14] the following naphthoquinone moieties have been selected (Figure²)²: 1,4-naphthoquinone, 2-chloro-1,4-naphthoquinone, 5-hydroxy-1,4-naphthoquinone (juglone). In analogy with the methoxy indanone scaffold of **1**, the 5- and 8-methoxy juglone derivatives were explored (Figure²)². 2-Methyl-1,4-naphthoquinone (menadione) was selected because of the reported potent differentiation activity toward neuronal progenitor cells of some derivatives.^[17]

Variations to the methylene linker have been also performed ($X=C=CH_2$ or NH). Finally, introduction of a methoxy group at position 4 of the benzyl ring was considered ($R^2=OCH_3$), on the basis of previous SAR studies.^[18]

To note, although several donepezil-based MTDLs have been developed (recently reviewed in^[19]), their design usually follows a framework combination strategy where the *N*-benzylpiperidine is combined with a second moiety carrying an extra AD-beneficial effect.

As discussed earlier,^[20] the multi-target drug discovery (MTDD) community has been over-reliant on the framework combination approach, sometimes overlooking that it may result in large hybrid structures and raise the so called “physicochemical challenge”^[21] typical of the field. This aspect is of particular importance when designing central nervous system (CNS)-directed MTDLs, which must first permeate the blood-brain barrier (BBB) to exert their multiple effects. Because of more stringent physicochemical requirements for CNS-acting drugs compared to peripherally acting compounds, the development of highly integrated, linker-less MTDLs holds particular promise.^[22]

In our case, **5--17** have been rationally designed by exploiting the existing structural similarity between the indanone and the naphthoquinone scaffold, which has allowed a fine amalgamation of the latter into the starting compound. In other words, the increase in molecular weight and change in physicochemical parameters of **5--17** are minimal with respect to **1** (Table^{^S1}). The high level of structural merging applied should ensure that **5--17** maintain the drug-like properties of a widely prescribed drug such is donepezil, while expanding its pharmacodynamic profile against AD.^[20]

Preliminary docking studies suggested that, in analogy with **1**, **5--17** could occupy both CAS and PAS of hAChE, forming contacts with multiple amino acid residues, such as W86, W286 and Y341 (Figure^{^S1}).

As a further important point in a multi-target perspective, our design approach builds on robust evidence of synergic effects provided by the combination of **1** and quinone drug idebenone (2-(10-hydroxydecyl)-5,6-dimethoxy-3-methylcyclohexa-2,5-diene-1,4-dione).^[23] The promising in^{^vivo} results reported for this combinatorial regimen represent a useful surrogate co-target validation for this project.^[24] In other words, they suggest that the simultaneous modulation of cholinesterase, amyloid and oxidative pathways might access context-specific multi-target mechanisms.

Synthesis

The reported methods of synthesizing N-linked quinones through classical SN₂ nucleophilic substitution reactions of 2-halo-derivatives with amines, or direct 1,4-type

addition of amines are quite flexible and reliable.^[25] This should allow the rapid preparation of diverse analogues and facilitate the medicinal chemistry activity.

Thus, for the preparation of 2-((1-benzylpiperidin-4-yl)amino)-1,4-naphthoquinones **5--16**, we reacted the proper naphthoquinone (**18--23**) with intermediate **24** or **25**, as depicted in Scheme^{^1}<schr1>.

First, benzylpiperidine synthons **24** and **25** were prepared by nucleophilic substitution of piperidin-4-one and the corresponding benzylchloride (**24^a** or **25^b**), with sodium carbonate in acetonitrile, at 70[°]C. Then, **24^b** and **25^b** were treated with ammonium acetate and sodium cyanoborohydride to provide 1-benzylpiperidin-4-amine derivatives **24** and **25** by a classical reductive amination.

2-Bromo-1,4-naphthoquinone (**18**), menadione (**22**) and 2,3-dichloro-1,4-naphthoquinone (**23**, dichlone) were commercially available, whereas 2-bromo-8-methoxy/hydroxy-1,4-naphthoquinones (**19**, **21**) and 2-bromo-5-methoxy-1,4-naphthoquinone (**20**) were synthesized according to published procedures.^[26] Then, reactions of piperidines **24** and **25** with **18--23** provided 2-substituted naphthoquinones **5--16** in low yield, mainly due to difficulties in the purification steps. To note, target compounds **5**^[27] and **10**^[28] were already reported for other applications and their characterization data are in agreement with those in the literature.

The synthesis of CH₂-linked target compound **17** posed some challenges, in view of the few precedents in the literature. Specifically, the synthetic route described in Scheme^{^2}<schr2> was followed. Commercially available 1-Boc-4-piperidylacetic acid **17a** was treated with menadione (**22**) in the presence of silver nitrate and ammonium persulfate, to obtain **17b** by a cross-coupling radical mechanism.^[29] *Tert*-butyloxycarbonyl protecting group was removed in acidic conditions by trifluoroacetic acid. Finally, deprotected **17c** was treated with benzyl chloride **24a** to provide the desired product **17** by nucleophilic substitution.

It should be noted that the radical reaction gave a very low yield (6[^]%) and resulted in a complex and quite inseparable mixture, probably because of a low stability of the intended primary alkyl radical intermediate that could undergo transposition to a more stable tertiary piperidyl radical. In fact, this reaction works well for linear carboxylic acid.^[30] Considering

this drawback and the fact that **17** proved to be moderately active (Table¹), no other medicinal chemistry efforts were performed in this direction.

Results and Discussion

As the first step of the multi-target characterization profile, all synthesized compounds were tested for their ability to inhibit human AChE and butyrylcholinesterase (hBuChE) by the colorimetric Ellman's assay (Table¹).^[31] The activities were expressed as IC₅₀ values and compared to those of donepezil (**1**), used as the reference compound. According to our expectations, all synthesized hybrids acted as ChE inhibitors. However, the replacement of the indanone with the naphthoquinone scaffold determined a general decrease of inhibitory activity towards AChE and a simultaneous shift in AChE/BuChE selectivity profile for selected compounds (**5**, **8--10**, **12**, **13** and **15**).

Regarding hAChE, all compounds, either carrying the NH or CH₂ linker, were less active than **1**. Particularly, introduction of the methoxy group on the benzyl ring provided derivatives **10--14**, which were all less potent than their respective unsubstituted compounds **16--19**. Thus, this modification on the piperidine fragment seems detrimental for anti-AChE activity. Incorporation of oxygenated substituents on the naphthoquinone differently affected hAChE inhibition; methoxy-derivatives **6** and **7** were the most potent within the series (IC₅₀ of 2.17^μM and 1.53^μM, respectively) and about one order of magnitude more potent than unsubstituted **5** (IC₅₀ equals to 22.6^μM). Conversely, the hydroxy derivatives **8** and **14** were inactive at the highest tested concentration (100^μM) or showed negligible activity, suggesting that this substitution is deleterious to hAChE recognition. Compounds **15** and **16** carrying a 3-Cl or a 3-Me naphthoquinone, together with a 4-methoxy-benzylpiperidine proved the less active of the series (no activity at 100^μM), indicating that the presence of an additional substituent at the 3-position hinders binding, presumably on steric grounds.

Remarkably, the results on the anti-hBuChE activity obtained for the performed modifications were more encouraging and disclosed potent and selective inhibitors of hBuChE. Evidence of an increased BuChE activity concomitant to a reduced expression of neuronal AChE during AD progression, the demonstration that BuChE can act as a surrogate for AChE in the brain, together with the fact that BuChE knockout mice show no phenotypic

abnormality, have validated BuChE as a preferred cholinergic target in the late disease stage.^[32] Indeed, experience with dual inhibitors suggests that BuChE inhibition is more efficient for increasing ACh levels in the AD brain and improving cognitive performance, with less parasympathetic side effects.^[33]

Intriguingly, the SAR for the two enzymes were quite divergent: this gives rise to several selective compounds.

The most active AChE inhibitor **7**, featuring a methoxy group in R³, resulted among the least active of the series (AChE/BuChE selectivity index >400). Differently from what observed for AChE, insertion of a methyl group in R² heavily impacted on anti-hBuChE activity, providing derivatives **9** and **15**, both endowed with remarkable sub-micromolar IC₅₀ values and high selectivity (selectivity indexes >400). The insertion of a methoxy group on the naphthoquinone fragment was beneficial only when combined with a 4-OMe-benzylpiperidine (*cf* **11--13** vs **5--7**).

The presence of the CH₂ linker did not affect activity in a significant way as concerns hAChE inhibition. **17** was nearly 6 times more active than **9**, and with a not-dissimilar IC₅₀ value compared to **5**. This is probably related to the fact that **17**, **9** and **5** show a quite similar arrangement of the naphthoquinone core and the benzylpiperidine when interacting with AChE. Conversely, compound **17** showed a modest IC₅₀ value for BuChE (equal to 28^μM), which is 295 times lower than that observed for the corresponding NH derivative **9**. Thus, a CH₂ linker is detrimental for BuChE activity.

Collectively, by combining potency and selectivity data from AChE/BuChE enzymatic screening, hits **7--9** and **15** were shortlisted for further assays.

In vitro blood-brain barrier permeation assay

In developing donepezil-derived MTDLs, BBB penetration is of great importance and should be checked at a very early stage of development. In the last years, the BBB parallel artificial membrane permeation assays (PAMPA-BBB) has established itself as a quick, high throughput and reliable in[^]vitro model for predicting passive BBB permeation. Thus, we used the PAMPA-BBB method to predict whether **7--9** and **15** could enter the brain

(Table²). In the same assay, drugs of known CNS penetration (including **1**) were tested, and their experimental values were compared to reported values, giving a good linear correlation. All the newly synthesized compounds showed positive permeability values. Particularly, **8** and **7** showed similar ($P_e=19.13\text{ cm}^{\text{s}^{-1}}$) or even higher ($P_e=25.73\text{ cm}^{\text{s}^{-1}}$) P_e values than that found for **1** ($P_e=21.93\text{ cm}^{\text{s}^{-1}}$). Thus, it is expected that **7**, **8**, but also **9** and **15**, could effectively penetrate into the CNS.

Cell-based profile: Cytotoxicity and neuroprotection

With these promising data on ChE inhibition and BBB permeation in hand, we established the cell-based profile of compounds **7--9** and **15**. Prior to any neuroprotection investigations, the cytotoxicity profile on the human liver cancer Hep-G2 (Figure³) and neuroblastoma SH-SY5Y (Figure⁴) cell lines were determined.

Lack of hepatotoxicity would be a critical determinant for the drug-likeness of new donepezil derivatives, as aging, comorbidity and subsequent polytherapy significantly increase the risk of liver injury in AD patients.^[35] As shown in Figure³, up to $5\text{ }\mu\text{M}$, there was no toxic effect from any of the molecules toward Hep-G2 cells, an established model for early ADME/Tox predictions.

At $10\text{ }\mu\text{M}$, the viability of cells treated with the juglone derivative **8** remained as high as $\geq 70\%$ compared to the untreated control cells. This supports the view that, in spite of the insertion of a quinone fragment (potentially hepatotoxic), **7**, **9** and **15** retain the favorable hepatotoxicity profile of **1**.^[36]

Next, we tested neuronal viability to rule out any possible neurotoxic effect of **7--9** and **15** (Figure⁴). This is motivated by the consideration that several AD drug candidates have failed due to neurotoxicity from a chronic treatment.^[37] Encouragingly, while **8** shows a dose-dependent decrease in cell viability, **7**, **9** and **15** display a quite safe neurotoxicity profile. In fact, the percentages of viable cells at the highest tested concentration were not different from that reported for **1** (70% at $10\text{ }\mu\text{M}$).^[38]

We expected that our quinone derivatives should be able to exert antioxidant effect and prevent neuronal cell death induced by reactive oxygen species (ROS). The deleterious

consequences of an excessive oxidation status and the pathophysiological role of ROS have been extensively studied in the context of AD.^[39] Neuronal cell dysfunction and oxidative cell death caused by the AD-associated A β peptide may causally contribute to the pathogenesis of AD.^[39]

Thus, we progressed **7**, **9** and **15**, for neuroprotection studies against oxidative stress. Clearly, juglone derivative **8** was discarded because of potential toxicity concerns (Figures³ and 4).

The antioxidant activity was evaluated against formation of ROS in SH-SY5Y neuronal-like cells in absence and presence of *t*BuOOH (TBH), an organic peroxide widely used to induce oxidative stress. Experiments were also performed with cells treated with sulforaphane (4-methylsulfinylbutyl isothiocyanate), an inducer of phase 2 enzyme NQO1. We have previously demonstrated that NQO1 extends the antioxidant potential of synthetic quinones through the generation of the corresponding hydroquinones, which represent the actual antioxidant species.^[14] Notably, an increase in NQO1 expression and activity has been shown in neurons and astrocytes of AD brains compared to age-matched normal controls, as a response to the oxidative stress of the AD process.^[40]

Intracellular ROS level were monitored by using 2',7'-dichlorodihydro-fluorescein diacetate (H2DCFDA). The nonfluorescent H2DCFDA is converted by ROS to the highly fluorescent 2',7'-dichlorofluorescein (DCF).

First, we verified whether treatment with redox-active **7**, **9** and **15** could alter the basal cell redox status. Positively, only a slight ROS increase with respect to the control was observed (Figure⁵).

On the other hand, a similar antioxidant activity was detected for **7**, **9** and **15**, following the oxidative stress provoked by TBH. However, all compounds were not able to fully restore the ROS levels back to the control (Figure⁶).

Interestingly, their antioxidant profile was boosted in the sulforaphane model, which should mimic the clinical pathological features of AD (i.e., an upregulation of NQO1 and

cell antioxidant system). Probably in virtue of the NQO1-mediated hydroquinone formation, 7, 9 and 15 were able to reduce the basal ROS level by more than 50% (Figure⁷).

Even more interestingly, they were able to completely reverse the toxic oxidative insult. As evident from Figure⁸, after TBH-induced oxidative stress and treatment with 7, 9 and 15, the ROS levels were similar to that of the untreated control.

Inhibition of A β ₄₂ aggregation

Quinones are effective modulators of aggregation of various amyloidogenic proteins.^[41] Hence, the ability of the most promising derivative 9 to inhibit the A β ₄₂ self-aggregation was assessed. Selection of 9 over 7 and 15 was based on its stronger anti-cholinesterase activity towards hBuChE, while showing safety profile and antioxidant activity similar to 7 and 15. Among the most abundant A β peptides, A β ₄₂ is the most prone to aggregate, as well as the most neurotoxic isoform; hence, inhibition of its aggregation is considered an effective avenue to limit the neurotoxic cascade of events associated with the formation of A β insoluble aggregates. Anti-aggregating properties of 9 were determined by a well-established thioflavin^T (ThT) fluorescence assay.^[42]

Derivative 9 significantly inhibited A β ₄₂ self-aggregation (52.0 \pm 8.0% inhibition when assayed at 1:1 ratio with A β ₄₂). Compared to the reference antiaggregating agent curcumin (diferuloylmethane), 9 resulted less potent by 30% (% inhibition by curcumin at 50 μ M=80.4 \pm 5.3), while its inhibitory activity was in line with that of 8-hydroxyquinoline derivatives which were generated by combining donepezil and clioquinol.^[34]

Conversely, and as previously reported,^[34] 1 was devoid of any significant anti-aggregating property (% inhibition at 50 μ M equals to 5.6 \pm 2.3%).

Neurotoxicity in primary neurons

Considering the well-known cytotoxicity mediated by quinones and to get further proof of the drug-likeness of 9, we tested its neurotoxicity against a primary cell line of cerebellar granule neurons (CGNs), widely used as a model for studying neuronal death in AD.^[35] Notwithstanding the notion that primary neurons are overall more sensitive to drug treatment than immortalized cell lines (e.g., SH-SY5Y), 9 showed a safe profile also in this

cell model (Figure⁹). The percentage of viable cells was >60% even at the highest tested concentration of 50 μ M. This result is remarkable, especially considering the high neurotoxicity shown by menadione, which is the quinone fragment of 9 (Figure^{S2}).

Conclusion

In conclusion, this paper describes our strategy to convert a first-line, symptomatic AD medication into a promising MTDL hit compound (9), with a potential disease-modifying profile. Thanks to a finely tuned MTDD rationale, a quinone-based donepezil derivative with concomitant antioxidant and anti-amyloid *in vitro* activities, combined with a desirable drug-like profile has been developed. The next milestone will be to test its *in vivo* efficacy.

Experimental Section

Chemistry

All commercially available reagents and solvents were purchased from Sigma-Aldrich, TCI, Alpha Aesar (Italy), and used without further purification. Reactions were followed by analytical thin layer chromatography (TLC), performed on precoated TLC plates (0.20 mm silica gel 60 with UV254 fluorescent indicator, Merck). Developed plates were air-dried and visualized by exposure to UV light (λ =254 nm and 365 nm). Reactions involving generation or consumption of amines were visualized using bromocresol green spray (0.04% in EtOH). Column chromatography purifications were performed under flash conditions using Sigma-Aldrich silica gel (grade 9385, 60 μ m, 230--400 mesh). NMR experiments were run on a Varian VXR400 (400 MHz for ¹H; 100 MHz for ¹³C). ¹H and ¹³C NMR spectra were acquired at 300 K using deuterated chloroform (CDCl₃) as solvent. Chemical shifts (δ) are reported in parts per million (ppm) relative to the residual solvent peak as an internal reference and coupling constants (*J*) are reported in hertz (Hz). Spin multiplicity is reported as: s=singlet, br s=broad singlet, d=doublet, dd=doublet of doublets, t=triplet, td=triplet of doublets, q=quartet, m=multiplet. Mass spectra were recorded on a Waters ZQ 4000, XevoG2-XSQTof, Acquity arc-QDA LC-MS apparatus with electrospray ionization (ESI) in positive mode. All final compounds are >90% pure, as judged by either HPLC, LC-MS, and NMR.

General procedure for the synthesis of 1-benzylpiperidin-4-ones (24^b and 25^b):

piperidin-4-one (1 equiv) and benzyl chloride 24^a or 25^a (1 equiv) were suspended in MeCN.

Sodium carbonate (4^{equiv}) was added to the suspension and the resulting mixture was stirred at 70^{°C} for 2^h. After cooling to room temperature, the mixture was filtered to remove solid materials and washed with MeCN. The solvent was evaporated under reduced pressure to afford the desired product (**24^b** or **25^b**) that was used for the next step without further purification.

1-Benzylpiperidin-4-one (24^b): Compound **24^b** was isolated as a colorless oil (yield: 826^{mg}, 45[%]): ¹H NMR (CDCl₃, 400^{MHz}): δ =2.44 (t, J =6,4^{Hz}, 4H), 2.73 (t, J =6,4^{Hz}, 4H), 3.61 (s, 2H), 7.33^{ppm} (m, 5H); ¹³C NMR (CDCl₃, 100^{MHz}): δ =41.3, 52.9, 62.0, 76.7, 77.0, 77.3, 138.1, 209.2^{ppm}.

1-(4-Methoxybenzyl)piperidin-4-one (25^b): Compound **25^b** was isolated as a colorless oil (yield: 315^{mg}, 45[%]): ¹H NMR (CDCl₃, 400^{MHz}): δ =2.43 (t, J =6,4^{Hz}, 4H), 2.71 (t, J =6,4^{Hz}, 4H), 3.55 (s, 2H), 3.79 (s, 3H), 6.86 (d, J =4,8^{Hz}, 2 H), 7.26^{ppm} (d, J =5,6^{Hz}, 2H); ¹³C NMR (CDCl₃, 100^{MHz}): δ =35.9, 48.8, 52.2, 55.2, 62.4, 113.5, 130.3, 130.4, 158.6^{ppm}.

General procedure for the synthesis of 1-benzylpiperidin-4-amine (24 and 25): NaBH₃CN (7.6^{equiv}) and CH₃COONH₄ (10^{equiv}) were added portion wise to a solution of 1-benzylpiperidin-4-one (**24^b** or **25^b**; 1^{equiv}) in MeOH and the resulting mixture was refluxed for 1^h. The solvent was removed in vacuo and water was added to the resulting residue. The aqueous mixture was acidified to pH² with HCl 2^N and stirred at room temperature for 15^{min}. Water was saturated by adding Na₂CO₃ and the desired product was extracted with AcOEt. The organic phase was dried over anhydrous Na₂SO₄, filtered and the solvent was removed under reduced pressure. The obtained crude material was purified by chromatography, by eluting with CH₂Cl₂/MeOH/NH₃ (9[:]1:0.1) to afford the title compound (**24** or **25**).

1-Benzylpiperidin-4-amine (24): Compound **24** was isolated as a yellowish oil (yield: 262^{mg}, 40[%]): ¹H NMR (CDCl₃, 400^{MHz}): δ =1.76 (d, J =12^{Hz}, 3H), 1.98 (t, J =12.4^{Hz}, 2 H), 2.77 (d, J =11.2^{Hz}, 4H), 3.45 (s, 2H), 7.22^{ppm} (m, 5H); ¹³C NMR (CDCl₃, 100^{MHz}): δ =41.3, 52.9, 62.0, 76.7, 77.0, 77.3, 138.1, 209.2^{ppm}.

1-(4-Methoxybenzyl)piperidin-4-amine (25): Compound **25** was isolated as a yellowish oil (yield: 302^{mg}, 40[%]): ¹H NMR (CDCl₃, 400^{MHz}): δ =1.38 (t, J =9.2^{Hz}, 2H), 1.78 (d, J =12.4^{Hz}, 2H), 1.96 (t, J =11.6^{Hz}, 2H), 2.63 (m, 1H), 2.82 (d, J =11.6^{Hz}, 2H), 3.42 (s, 2H),

3.77 (s, 3H), 6.83 (d, $J=8.8$ Hz, 2H), 7.20 ppm (d, $J=8.8$ Hz, 2H); ^{13}C NMR (CDCl_3 , 100 MHz): $\delta=35.9, 48.8, 52.2, 55.2, 62.4, 113.5, 130.3, 130.4, 158.6$ ppm.

General procedure for the synthesis of 2-((1-benzylpiperidin-4-yl)amino)naphthalene-1,4-dione (5--8, 10--14, 16): 1-Benzylpiperidin-4-amine **24** or **25** (1 equiv) was added to a solution in DMF or MeOH of the corresponding naphthoquinone (**18--23**; 1 equiv). The resulting mixture was stirred at room temperature for 1--2 h (monitoring by TLC).

After reaction completion, MeOH was removed under reduced pressure; in case of reaction performed in DMF, the solvent was eliminated by extraction with LiCl 5% solution and CH_2Cl_2 . The organic phase was dried over anhydrous Na_2SO_4 , filtered, and solvent evaporated under reduced pressure. For the synthesis of compounds **5--8, 11--14, 16**, the obtained crude material was purified by column chromatography, whereas for compounds **6, 7** and **14**, a further recrystallization from MeOH was performed. Compound **10** was purified by washing the crude with diethyl ether, followed by recrystallization from EtOH.

2-((1-Benzylpiperidin-4-yl)amino)naphthalene-1,4-dione (5): Purification by chromatography ($\text{CH}_2\text{Cl}_2/\text{EtOH}$ 9.8:0.2) afforded title compound **5** as an orange solid (yield: 14 mg, 8%): ^1H NMR (CDCl_3 , 400 MHz): $\delta=1.64$ (m, 2H), 2.05 (d, $J=11.6$ Hz, 2H), 2.20 (t, $J=10.4$ Hz, 2H), 2.87 (d, $J=10.4$ Hz, 2H), 3.31 (m, 1H), 3.53 (s, 2H), 5.75 (s, 1H), 5.84 (d, $J=7.7$ Hz, NH), 7.32 (m, 5H), 7.60 (td, $J=7.6$ Hz, 1H), 7.71 (td, $J=7.6$ Hz, 1H), 8.04 (dd, $J=7.7$ Hz, 1H), 8.09 ppm (dd, $J=7.7$ Hz, 1H); ^{13}C NMR (CDCl_3 , 100 MHz): $\delta=31.1, 51.8, 62.9, 101.8, 126.1, 126.3, 127.1, 128.3, 129.1, 132.0, 134.8, 146.7, 183.0, 183.7$ ppm; MS (ESI^+) m/z 347 $[M+\text{H}]^+$.

2-((1-Benzylpiperidin-4-yl)amino)-8-methoxynaphthalene-1,4-dione (6): Purification by chromatography ($\text{CH}_2\text{Cl}_2/\text{EtOH}$ 9.8:0.2) and further recrystallization from MeOH afforded title compound **6** as an orange solid (yield: 62 mg, 30%): ^1H NMR (CDCl_3 , 400 MHz): $\delta=1.63$ (d, $J=10$ Hz, 2H), 2.03 (d, $J=11.2$ Hz, 2H), 2.21 (t, $J=9.6$ Hz, 2H), 2.84 (d, $J=11.2$ Hz, 2H), 3.31 (m, 1H), 3.52 (s, 2H), 4.00 (s, 3H), 5.69 (s, 1H), 6.01 (d, $J=6.8$ Hz, NH), 7.19 (d, $J=8.8$ Hz, 1H), 7.32 (m, 5H), 7.69 (t, $J=8$ Hz, 1H), 7.79 ppm (d, $J=8.4$ Hz, 1H); ^{13}C NMR (CDCl_3 , 100 MHz): $\delta=31.2, 49.5, 51.9, 63.0, 101.1, 126.2, 126.4, 127.2, 128.4, 129.1, 130.6, 132.0, 133.7, 134.8, 138.1, 146.8, 182.0, 183.0$ ppm.

2-((1-Benzylpiperidin-4-yl)amino)-5-methoxynaphthalene-1,4-dione (7): Purification by chromatography (CH₂Cl₂/EtOH 9.8:0.2) and further recrystallization from MeOH, afforded title compound **7** as a yellow oil (yield: 52^{mg}, 25[%]): ¹H NMR (CDCl₃, 400^{MHz}): δ 1.63 (d, J =10^{Hz}, 2H), 2.03 (d, J =11,2^{Hz}, 2H), 2.21 (t, J =9,6^{Hz}, 2H), 2.84 (d, J =11,2^{Hz}, 2H), 3.31 (m, 1H), 3.52 (s, 2H), 4.00 (s, 3H), 5.69 (s, 1H), 6.01 (d, J =6,8^{Hz}, NH), 7.19 (d, J =8,8^{Hz}, 1H), 7.32 (m, 5H), 7.69 (t, J =8^{Hz}, 1H), 7.79^{ppm} (d, J =8,4^{Hz}, 1H); ¹³C NMR (CDCl₃, 100^{MHz}): δ 31.0, 51.7, 56.4, 63.1, 99.6, 115.8, 119.0, 127.1, 128.3, 129.0, 136.0, 147.6, 160.2, 180.3, 182.4^{ppm}. MS (ESI⁺) m/z 377 [$M+H$]⁺.

2-((1-Benzylpiperidin-4-yl)amino)-8-hydroxynaphthalene-1,4-dione (8): Purification by chromatography (CH₂Cl₂/EtOH/NH₃ 9.8:0.2:0.05) afforded title compound **8** as a red solid (yield: 30^{mg}, 15[%]): ¹H NMR (CDCl₃, 400^{MHz}): δ 1.67 (d, J =10^{Hz}, 2H), 2.04 (d, J =11,6^{Hz}, 2H), 2.21 (t, J =10,8^{Hz}, 2H), 2.88 (d, J =12^{Hz}, 2H), 3.34 (m, 1H), 3.53 (s, 2H), 5.64 (s, 1H), 6.02 (d, J =7,2^{Hz}, NH), 7.35 (m, 6H), 7.48 (t, J =8^{Hz}, 1H), 7.60 (d, J =7,2^{Hz}, 1H), 13.05^{ppm} (s, OH); ¹³C NMR (CDCl₃, 100^{MHz}): δ 29.9, 30.9, 49.6, 51.6, 62.8, 99.9, 114.8, 119.1, 125.9, 127.3, 128.3, 129.1, 130.5, 133.9, 147.4, 161.0, 181.1, 188.9^{ppm}. MS (ESI⁺) m/z 363 [$M+H$]⁺.

2-((1-Benzylpiperidin-4-yl)amino)-3-chloronaphthalene-1,4-dione (10): Recrystallization from EtOH afforded title compound **10** as an orange solid (yield: 50^{mg}, 33[%]): ¹H NMR (CDCl₃, 400^{MHz}): δ 1.67 (d, J =10.4^{Hz}, 2H), 2.06 (d, J =12^{Hz}, 2H), 2.22 (t, J =11.2^{Hz}, 2H), 2.89 (d, J =11.2^{Hz}, 2H), 3.56 (s, 2H), 4.45--4.43 (m, 1H), 5.99 (s, NH), 7.32--7.24 (m, 5H), 7.59 (t, J =7.6^{Hz}, 1H), 7.69 (t, J =7.2^{Hz}, 1H), 8.00 (d, J =7.2^{Hz}, 1H), 8.11 (d, J =7.2^{Hz}, 1H); ¹³C NMR (CDCl₃, 100^{MHz}): δ 33.7, 50.7, 51.8, 62.9, 127.0, 127.5, 128.5, 129.4, 129.9, 132.6, 132.8, 135.1, 143.5, 177.0, 180.4, ppm; MS (ESI⁺) m/z 381 [$M+H$]⁺.

8-Methoxy-2-((1-(4-methoxybenzyl)piperidin-4-yl)amino)naphthalene-1,4-dione (11): Purification by chromatography (CH₂Cl₂/EtOH 9.8:0.2) afforded title compound **11** as an orange solid (yield: 27^{mg}, 13[%]): ¹H NMR (CDCl₃, 400^{MHz}): δ 1.64 (d, J =7.2^{Hz}, 2H), 2.04 (d, J =11.8^{Hz}, 2H), 2.17 (t, J =10.8^{Hz}, 2H), 2.85 (d, J =12^{Hz}, 2H), 3.36 (m, 1H), 3.46 (s, 2H), 3.80 (s, 3H), 5.74 (s, 1H), 5.83 (d, J =7.6^{Hz}, NH), 6.87 (d, J =6.4^{Hz}, 2H), 7.26 (m, 2H), 7.63 (t, J =8^{Hz}, 1H), 7.74 (t, J =8^{Hz}, 1H), 8.05 (d, J =12^{Hz}, 1H), 8.10^{ppm} (d, J =11.6^{Hz}, 1H); ¹³C

NMR (CDCl₃, 100[^]MHz): <Gd>=31.1, 51.7, 49.8, 55.2, 62.3, 101.0, 113.6, 126.1, 126.3, 130.2, 131.9, 133.9, 134.7, 146.7, 183.0, 183.7[^]ppm; MS (ESI⁺) *m/z* 377 [M+H]⁺.

8-Methoxy-2-((1-(4-methoxybenzyl)piperidin-4-yl)amino)naphthalene <M->1,4-dione

(12): Purification by chromatography (CH₂Cl₂/EtOAc/EtOH 5[^]:4.8:0.2) afforded title compound **12** as a yellow solid (yield: 32[^]mg, 14[^]%): ¹H NMR (CDCl₃, 400[^]MHz): <Gd>=1.62 (d, *J*=10.4[^]Hz, 2H), 2.02 (d, *J*=10.4[^]Hz, 2H), 2.19 (t, *J*=10.4[^]Hz, 2H), 2.82 (d, *J*=11.6[^]Hz, 2H), 3.30 (m, 1H), 3.46 (s, 2H), 3.80 (s, 3H), 4.00 (s, 3H), 5.68 (s, 1H), 5.10 (d, *J*=8[^]Hz, NH), 6.88 (d, *J*=4.8[^]Hz, 2H), 7.21 (m, 3H), 7.68 (t, *J*=7.2[^]Hz, 1H), 7.79[^]ppm (d, *J*=8[^]Hz, 1H); ¹³C NMR (CDCl₃, 100[^]MHz): <Gd>=31.0, 51.5, 55.2, 56.4, 62.3, 99.4, 113.6, 115.8, 118.5, 119.0, 130.2, 136.0, 136.1, 147.6, 158.8, 160.1, 180.4, 182.4[^]ppm.

5-Methoxy-2-((1-(4-methoxybenzyl)piperidin-4-yl)amino)naphthalene <M->1,4-dione

(13): Purification by chromatography (CH₂Cl₂/EtOH 9.8:0.2) afforded title compound **13** as a yellowish solid (yield: 56[^]mg, 25[^]%): ¹H NMR (CDCl₃, 400[^]MHz): <Gd>=1.62 (d, *J*=10.4[^]Hz, 2H), 2.02 (d, *J*=10.4[^]Hz, 2H), 2.19 (t, *J*=10.4[^]Hz, 2H), 2.82 (d, *J*=11.6[^]Hz, 2H), 3.30 (m, 1H), 3.46 (s, 2H), 3.80 (s, 3H), 4.00 (s, 3H), 5.68 (s, 1H), 5.10 (d, *J*=8[^]Hz, NH), 6.88 (d, *J*=4.8[^]Hz, 2H), 7.21 (m, 3H), 7.68 (t, *J*=7.2[^]Hz, 1H), 7.79[^]ppm (d, *J*=8[^]Hz, 1H); ¹³C NMR (CDCl₃, 100[^]MHz): <Gd>=31.0, 51.5, 55.2, 56.3, 62.4, 99.4, 113.6, 115.8, 119.0, 130.0, 131.4, 136.0, 147.6, 158.8, 160.1, 180.3, 182.4[^]ppm.

8-Hydroxy-2-((1-(4-methoxybenzyl)piperidin-4-yl)amino)naphthalene-1,4-dione (14):

Purification by chromatography (CH₂Cl₂/EtOH/NH₃ 9.8:0.2:0.05) and further recrystallization from MeOH, afforded title compound **14** as a yellowish solid (yield: 35[^]mg, 16[^]%): ¹H NMR (CDCl₃, 400[^]MHz): <Gd>=1.62 (d, *J*=10[^]Hz, 2H), 2.04 (d, *J*=11.2[^]Hz, 2H), 2.17 (t, *J*=10.4[^]Hz, 2H), 2.87, (d, *J*=9.2[^]Hz, 2H), 3.36 (m, 1H), 3.48 (s, 2H), 3.81 (s, 3H), 5.64 (s, 1H), 6.01 (d, *J*=7.2[^]Hz, NH), 6.88 (d, *J*=7.6[^]Hz, 2H), 7.25 (m, 3H), 7.48 (t, *J*=8[^]Hz, 1H), 7.60 (d, *J*=7.6[^]Hz, 1H), 13.05[^]ppm (s, OH); ¹³C NMR (CDCl₃, 100[^]MHz): <Gd>=31.0, 47.4, 51.5, 55.2, 62.4, 99.4, 113.7, 119.1, 125.9, 130.2, 133.8, 147.4, 161.0, 182.4, 189.1[^]ppm.

2-Chloro-3-((1-((4-(1-hydroperoxy-113-ethyl)phenyl)methyl)piperidin-4-yl)amino)

naphthal-ene-1,4-dione (16): Recrystallization from EtOH afforded title compound **16** as an orange solid (yield: 75[^]mg, 33[^]%): ¹H NMR (CDCl₃, 400[^]MHz): <Gd>=1.64 (d, *J*=10.8[^]Hz, 2H), 2.08

(d, $J=10.8$ Hz, 2H), 2.19 (t, $J=11.6$ Hz, 2H), 2.87 (d, $J=10.4$ Hz, 2H), 3.48 (s, 2H), 3.80 (s, 3H), 4.26 (m, 1H), 6.01 (d, $J=7.2$ Hz, NH), 6.87 (d, $J=8$ Hz, 2H), 7.24 (m, 2H), 7.64 (t, $J=1.2$ Hz, 1H), 7.72 (t, $J=1.2$ Hz, 1H), 8.04 (d, $J=7.2$ Hz, 1H), 8.15 ppm (d, $J=7.2$ Hz, 1H); ^{13}C NMR (CDCl_3 , 100 MHz): δ =33.8, 50.8, 51.5, 55.2, 62.3, 113.8, 126.8, 130.3, 132.4, 134.9, 143.3, 158.8, 180.5 ppm.

General procedure for the synthesis of 2-((1-benzylpiperidin-4-yl)amino)naphthalene-1,4-dione (9, 15): 1-benzylpiperidin-4-amine **24** or **25** (1 equiv) was added to a solution of 2-methylnaphthalene-1,4-dione (**22**; 1 equiv) in EtOH. The resulting mixture was stirred at room temperature for 2 h, while monitoring the reaction by TLC. The solvent was removed under reduced pressure and the crude material was purified by chromatography followed by a recrystallization from EtOH.

2-((1-Benzylpiperidin-4-yl)amino)-3-methylnaphthalene-1,4-dione (9): Purification by chromatography (CH_2Cl_2 /toluene/EtOAc/EtOH 8:1:0.7:0.3) and further recrystallization from EtOH afforded title compound **9** as a red solid (yield: 14 mg, 7%): ^1H NMR (CDCl_3 , 400 MHz): δ =1.14 (d, $J=5.6$ Hz, 2H), 1.62 (d, $J=10.4$ Hz, 2H), 1.99 (t, $J=12$ Hz, 2H), 2.17 (s, 3H), 2.85 (d, $J=12$ Hz, 2H), 3.53 (s, 2H), 3.69--3.85 (m, 1H), 5.69 (d, $J=9.2$ Hz, NH), 7.21--7.33 (m, 5H), 7.59 (t, $J=7.2$ Hz, 1H), 7.69 (t, $J=7.2$ Hz, 1H), 8.01 (d, $J=7.2$ Hz, 1H), 8.09 ppm (d, $J=7.2$ Hz, 1H); ^{13}C NMR (CDCl_3 , 100 MHz): δ =11.3, 33.8, 51.7, 62.9, 126.0, 126.2, 127.1, 128.2, 129.1, 131.9, 134.3, 145.3, 180.3, 182.4 ppm. HRMS (ESI^+) calcd for $\text{C}_{23}\text{H}_{24}\text{N}_2\text{O}_2$ [$M+\text{H}$] $^+$ 361.1911, found 361.1910.

2-((1-(4-Methoxybenzyl)piperidin-4-yl)amino)-3-methylnaphthalene-1,4-dione (15): Purification by chromatography (CH_2Cl_2 /MeOH 9:1) and further recrystallization from EtOH afforded title compound **15** as a red oil (yield: 11 mg, 5%): ^1H NMR (CDCl_3 , 400 MHz): δ =1.70--1.50 (m, $J=9.9$ Hz, 4H), 1.96 (d, $J=12.3$ Hz, 2H), 2.12 (d, $J=11.2$ Hz, 1H), 2.16 (s, $J=15.3$ Hz, 3H), 2.83 (d, $J=11.4$ Hz, 2H), 3.47 (s, 2H), 3.80 (s, 3H), 5.67 (d, $J=9.2$ Hz, NH), 6.86 (d, $J=8.6$ Hz, 2H), 7.22 (d, $J=8.5$ Hz, 2H), 7.60--7.53 (m, 1H), 7.67 (td, $J=7.6, 1.1$ Hz, 1H), 7.99 (d, $J=7.6$ Hz, 1H), 8.08 (d, $J=7.7$ Hz, 1H); ^{13}C NMR (CDCl_3 , 100 MHz): δ =11.4, 23.0, 33.9, 51.2, 51.7, 55.4, 62.4, 68.5, 113.8, 126.2, 126.4, 130.4, 130.5, 132.0, 133.6, 134.4, 145.4, 158.9, 182.7, 183.6 ppm. MS (ESI^+) m/z 391 [$M+\text{H}$] $^+$.

tert-Butyl 4-((3-methyl-1,4-dioxo-1,4-dihydronaphthalen-2-yl)methyl)piperidine-1-carboxylate (17^b): In a two-neck flask 2-(1-(tert-butoxycarbonyl)piperidin-4-yl)acetic acid (17^a; 3^{equiv}) and AgNO₃ (0.3^{equiv}) were added to a solution of menadione (1^{equiv}) in a mixture of MeCN/H₂O (2[^]:1) heated to 65[°]C. When a clear solution was obtained, a 0.38^M solution of (NH₄)₂S₂O₈ (1.3^{equiv}) in MeCN/H₂O was added dropwise in 1^h. The resulting mixture was refluxed for 5^h. The solvents were removed in vacuo and the resulting crude was purified by chromatography, eluting with petroleum ether/EtOAc (9[^]:1) to afford the title compound. Compound 17^b was obtained as a yellow solid (yield: 6^{mg}, 6[%]): ¹H NMR (CDCl₃, 400^{MHz}): <Gd>=1.44 (s, 9H); 1.66--1.54 (m, 4H), 1.79--1.66 (m, 1H), 2.19 (s, 3H), 2.67--2.50 (m, 4H), 4.08 (m, 2H), 7.69 (d, *J*=11.9^{Hz}, 2H), 8.07^{ppm} (d, *J*=13.3^{Hz}, 2H); ¹³C NMR (CDCl₃, 100^{MHz}): <Gd>=13.36, 28.42, 29.65, 33.69, 36.57, 43.88, 79.22, 126.23, 126.33, 132.03, 132.11, 133.48, 144.51, 145.13, 154.90, 184.86, 185.05^{ppm}; MS (ESI⁺) *m/z* 761.2 [*M*+Na]⁺.

2-((1-Benzylpiperidin-4-yl)methyl)-3-methylnaphthalene-1,4-dione (17): To a cooled (5[°]C, ice bath) solution of tert-butyl 4-((3-methyl-1,4-dioxo-1,4-dihydronaphthalen-2-yl)methyl)piperidine-1-carboxylate (17^b; 1^{equiv}) in CH₂Cl₂, TFA (3^{equiv}) was added dropwise. The cold bath was removed, and the reaction mixture was stirred at room temperature for 5^h. The solvent and the excess of TFA were removed in vacuo, and the resulting solid was washed with ethyl ether (x 3). The title compound 17^c was used in the next step without further purification. A 1.1^M solution of benzaldehyde (10^{equiv}) in dry MeOH was added to a 0.1^M solution of 17^c (1^{equiv}) and KOH (0.17^{equiv}) in dry MeOH (pH⁴⁻⁻⁵), the resulting mixture was refluxed for 15^{min}. After cooling the reaction to room temperature, NaBH₃CN (1^{equiv}) was added, and the mixture was stirred at room temperature for 5^h. The solvent was removed in vacuo and the resulting crude was purified by chromatography, eluting with CH₂Cl₂/MeOH (9[^]:1). The title compound 17 was obtained as a yellowish oil (yield: 6^{mg}, 30[%]): ¹H NMR (CDCl₃, 400^{MHz}): <Gd>=1.94--1.64 (m, 5H), 2.23--2.13 (m, 7H), 2.66 (d, *J*=6.8^{Hz}, 2H), 3.50--3.35 (m, 2H), 4.11 (s, 2H), 7.46--7.39 (m, 3H), 7.57--7.52 (m, 2H), 7.75--7.65 (m, 2H), 8.05--7.97 (m, 1H), 8.12--8.04^{ppm} (m, 1H); HRMS (ESI⁺) calcd for C₂₄H₂₅NO₂ [*M*+H]⁺ 360.1958, found 360.1921.

Biological methods

Human AChE and BuChE inhibition assay. AChE inhibitory activity was evaluated spectrophotometrically at 37°C by Ellman's method^[31] using a Jasco V-530 double beam spectrophotometer. The rate of increase in absorbance at 412 nm was followed for 240 s. An AChE stock solution was prepared by dissolving human recombinant AChE (EC: 3.1.1.7) lyophilized powder (Sigma-Aldrich) in 0.1 M potassium phosphate buffer (pH 8.0) containing Triton X-100 (0.1%). A stock solution of BuChE (EC: 3.1.1.8) from human serum (Sigma-Aldrich) was prepared by dissolving the lyophilized powder in an aqueous solution of gelatin (0.1%). Stock solutions of inhibitors (2 mM) were prepared in MeOH. The assay solution consisted of a 0.1 M potassium phosphate buffer (pH 8.0), with the addition of 5,5'-dithiobis(2-nitrobenzoic acid; 340 μM), human recombinant AChE or human serum BuChE (0.02 U/mL, Sigma-Aldrich), and substrate (550 μM acetylthiocholine iodide or butyrylthiocholine iodide, respectively). Fifty microliter aliquots of increasing concentrations of the test compound were added to the assay solution and pre-incubated for 20 min at 37°C with the enzyme, prior addition of substrate. Assays were carried out with a blank mixture containing all components except AChE or BuChE to account for non-enzymatic reactions. The reaction rates were compared, and the percent inhibition due to the presence of tested inhibitor at increasing concentrations was calculated. Each concentration was analyzed in triplicate, and IC₅₀ values were determined graphically from log concentration-inhibition curves (GraphPad Prism 4.03 software, GraphPad Software).

Inhibitory potency on Aβ₄₂ self-aggregation: Aβ₄₂ samples (Bachem AG, Switzerland) pre-treated with 1,1,1,3,3,3-hexafluoropropan-2-ol (HFIP) were solubilized with a CH₃CN/Na₂CO₃ (0.3 mM)/NaOH (250 mM; 48.4:48.4:3.2) mixture to obtain a stable stock solution ([Aβ₄₂]=500 μM).^[42,43] Experiments were performed by incubating the peptide in 10 mM phosphate buffer (pH 8.0) containing 10 mM NaCl at 30°C for 24 h (final Aβ concentration=50 μM) with and without inhibitors at 50 μM (Aβ/inhibitor=1:1). Blank solutions containing the tested inhibitors without Aβ₄₂ were also prepared and tested. To quantify amyloid fibril formation, the ThT fluorescence method was used.^[43] After incubation, samples were diluted to a final volume of 2.0 mL with 50 mM glycine-NaOH buffer (pH 8.5) containing 1.5 mM ThT. A 300-s time scan of fluorescence intensity was carried out (λ_{ex}=446 nm; λ_{em}=490 nm), and plateau values were averaged after subtracting the background fluorescence of the ThT solution. The fluorescence

intensities were compared, and the percent inhibition due to the presence of the tested inhibitor was calculated.

Cytotoxicity assays in cell lines. Human hepatocarcinoma Hep-G2[^] cell line and human neuroblastoma SH-SY5Y cell line were cultured in DMEM supplemented with 10[^]% FBS, 100 UI mL^{<M>¹} penicillin, 100[^]mg[^]mL^{<M>¹} streptomycin, in a 5[^]% CO₂ atmosphere at 37[^]°C, with saturating humidity. Cytotoxicity of selected compounds was estimated using an MTT-based assay.^[44] Briefly, cells were seeded in 96-well plates at a density of 5×10³ cells/well and incubated overnight at 37[^]°C, 5[^]% CO₂ in humidified atmosphere to allow adhesion. After this time, cells were treated for 24[^]h with compounds **7--9** and **15**, or vehicle (DMSO) at different concentrations. Then, cells were washed with PBS and treated with 300[^]μM MTT dissolved in DMEM and incubated for two hours at 37[^]°C and 5[^]% CO₂. After this time, the medium was removed, and the formazan salts were dissolved in DMSO. The formazan absorbance from each well was measured at λ=570[^]nm by using a microplate reader (Enspire, PerkinElmer).

Determination of antioxidant activity in SH-SY5Y cells. To evaluate the antioxidant activity of the selected compounds, SH-SY5Y cells were seeded in 96-well plates (OptiPlate black, PerkinElmer) at 5×10³ cells/well and incubated overnight at 37[^]°C, 5[^]% CO₂ to allow adhesion. To induce the expression of NQO1, cells were treated after adhesion with 4-methylsulfinylbutyl isothiocyanate (2.5[^]μM; Sigma-Aldrich) for 24[^]h. For oxidative stress determination, cells were treated for 24[^]h with the selected compounds or vehicle (DMSO). After this time, cells were washed with PBS and stained for 30[^]min with 10[^]μM H2DCFDA probe (2',7'-dichlorodihydrofluorescein diacetate, ThermoFisher) in DMEM. To induce oxidative stress, cells were carefully washed and treated for 30[^]min with 100[^]μM TBH (*tert*-butyl hydroperoxide solution, Luperon, Sigma-Aldrich) dissolved in DMEM. Finally, cells were washed three times with PBS supplemented with glucose 5[^]mM and CaCl₂ 1[^]mM. The DCF fluorescence was measured (<G>_{ex}=485[^]nm; <G>_{em}=535[^]nm) by using a microplate reader (Enspire, Perkin Elmer).

Cytotoxicity assays in primary neurons. Primary cultures of cerebellar granule neurons (CGNs) were prepared from 7-day-old pups of Wistar rat strain, as previously described.^[35] All animal experiments were authorized by the University of Bologna bioethical committee (protocol no. 17--72-1212) and performed according to Italian and European Community laws on the use of animals for

experimental purposes. Cells were dissociated from cerebella and plated on 96-well plates, previously coated with 10 µg/mL poly-L-lysine, at a density of 1.2×10^5 cells/0.2 mL medium/well in BME supplemented with 100 mL/L heat-inactivated FBS (Aurogene), 2 mmol/L glutamine, 100 µmol/L gentamicin sulphate and 25 mmol/L KCl (all from Sigma--Aldrich). 16 h later, 10 µM cytosine arabino-furanoside (Sigma--Aldrich) was added to avoid glial proliferation. After 7 days in vitro, differentiated neurons were shifted to serum free BME medium containing 25 mmol/L KCl and treated with increasing concentrations of the compounds (0, 1, 2.5, 5, 10, 25 and 50 µM) for 24 h. After 24 h of treatment, the viability of CGNs was evaluated through the MTT assay.

PAMPA-BBB Assay. In order to predict passive BBB penetration of novel compounds modification of the PAMPA has been used based on a reported protocol.^[45] The filter membrane of the donor plate was coated with PBL (Polar Brain Lipid, Avanti, AL, USA) in dodecane (4 µL of 20 mg/mL PBL in dodecane) and the acceptor well was filled with 300 µL of PBS pH 7.4 buffer (VA). Tested compounds were dissolved first in DMSO and that diluted with PBS pH 7.4 to reach the final concentration in the range between 40--100 µM in the donor well. Concentration of DMSO did not exceed 0.5% (v/v) in the donor solution. 300 µL of the donor solution was added to the donor wells (VD) and the donor filter plate was carefully put on the acceptor plate so that coated membrane was “in touch” with both donor solution and acceptor buffer. Test compound diffused from the donor well through the lipid membrane (Area=0.28 cm²) to the acceptor well. The concentration of the drug in both donor and the acceptor wells were assessed after 3, 4, 5 and 6 h of incubation in quadruplicate using the UV plate reader Synergy HT (Biotek, Winooski, VT, USA) at the maximum absorption wavelength of each compound. Besides that, solution of theoretical compound concentration, simulating the equilibrium state established if the membrane were ideally permeable was prepared and assessed as well. Concentration of the compounds in the donor and acceptor well and equilibrium concentration were calculated from the standard curve and expressed as the permeability (P_e) according the equation^[46]:

$$P_e = C \times \ln \left(1 - \frac{[drug]_{acceptor}}{[drug]_{equilibrium}} \right) \quad (2)$$

$$where C = \frac{(V_D \times V_A)}{(V_D \times V_A) Area \times Time}$$

The measurement predicts that the test compounds have the potential to passively pass the BBB. P_e values correspond to those of standard drugs with high CNS permeability.

Acknowledgements

This work was supported by the <cgs>University of Bologna (Italy)</cgs>, Fondazione Carisbo-Bando Internazionalizzazione 2019 (ASTROFARMA), <cgs>Czech Health Research</cgs> Council no. <cgcn>NU20-08-00296</cgcn>, <cgs>Ministry of Education, Youth and Sports of Czech Republic</cgs> (project ERDF no. <cgcn>CZ.02.1.01/0.0/0.0/18<?_>069/0010054</cgcn>) and student project no. <cgcn>SV/FVZ2020010</cgcn>. F.D.P. is grateful to the “Torno Subito” Programme, promoted by the <cgs>Regione Lazio</cgs>. We also acknowledge Maria Teresa Molina (CSIC, Spain) for providing initial samples of **19--21** and Alessandra Tolomelli for LC--MS. Elisa Liardo, Giulio Caldarelli, Alexia Mattellone are thanked for their technical assistance with compound synthesis.

Conflict of Interest

The authors declare no conflict of interest.

<lit1><other><https://www.euro.who.int/en/healthtopics/noncommunicable-diseases/mental-health/areas-of-work/dementia></other>.

<lit2><jnl><?><?>authors?<?><?> *Alzheimer's & Dementia* **2020**, *16*, 391--460</jnl>.

<lit3><jnl>J. Cummings, G. Lee, A. Ritter, M. Sabbagh, K. Zhong, *Alzheimer's Dementia* **2019**, *5*, 272--293</jnl>.

<lit4><jnl>L.[^]K. Huang, S.[^]P. Chao, C.[^]J. Hu, *J. Biomed. Sci.* **2020**, *27*, 18</jnl>.

<lit5><jnl>M.[^]L. Bolognesi, *Future Med. Chem.* **2017**, *9*, 707--709</jnl>.

<lit6><jnl>F. Mangialasche, A. Solomon, B. Winblad, P. Mecocci, M. Kivipelto, *Lancet Neurol.* **2010**, *9*, 702--716</jnl>.

<lit7><jnl>J. Birks, *Cochrane Database Syst Rev* **2006**, CD005593</jnl>.

<lit8><jnl>J.[^]T. Brewster, S. Dell'Acqua, D.[^]Q. Thach, J.[^]L. Sessler, *ACS Chem. Neurosci.* **2019**, *10*, 155--167</jnl>.

- <lit9><lit_a><jnl>A. Cavalli, M.[^]L. Bolognesi, A. Minarini, M. Rosini, V. Tumiatti, M. Recanatini, C. Melchiorre, *J. Med. Chem.* **2008**, *51*, 347--372</jnl>;
- <lit_b><jnl>M.[^]L. Bolognesi, A. Cavalli, *ChemMedChem* **2016**, *11*, 1190--1192</jnl>.
- <lit10><lit_a><jnl>M. Bajda, N. Guzior, M. Ignasik, B. Malawska, *Current Med Chem* **2011**, *18*, 4949--4975</jnl>; <lit_b><jnl>R. León, A.[^]G. Garcia, J. Marco-Contelles, *Med. Res. Rev.* **2013**, *33*, 139--189</jnl>; <lit_c><jnl>K.[^]S. Dias, C. Viegas, *Curr. Neuropharmacol.* **2014**, *12*, 239--255</jnl>; <lit_d><jnl>L. Ismaili, B. Refouvelet, M. Benchekroun, S. Brogi, M. Brindisi, S. Gemma, G. Campiani, S. Filipic, D. Agbaba, G. Esteban, M. Unzeta, K. Nikolic, S. Butini, J. Marco-Contelles, *Prog. Neurobiol.* **2017**, *151*, 4--34</jnl>; <lit_e><jnl>R.[^]R. Ramsay, M.[^]R. Popovic-Nikolic, K. Nikolic, E. Uliassi, M.[^]L. Bolognesi, *Clin Transl Med* **2018**, *7*, 3</jnl>; <lit_f><jnl>Q. Li, S. He, Y. Chen, F. Feng, W. Qu, H. Sun, *Eur. J. Med. Chem.* **2018**, *158*, 463--477</jnl>; <lit_g><jnl>E. Mezeiova, K. Chalupova, E. Nepovimova, L. Gorecki, L. Prchal, D. Malinak, K. Kuca, O. Soukup, J. Korabecny, *Curr. Alzheimer Res.* **2019**, *16*, 772--800</jnl>.
- <lit11><lit_a><jnl>M. Rosini, E. Simoni, A. Milelli, A. Minarini, C. Melchiorre, *J. Med. Chem.* **2014**, *57*, 2821--2831</jnl>; <lit_b><jnl>M. Unzeta, G. Esteban, I. Bolea, W.[^]A. Fogel, R.[^]R. Ramsay, M.[^]B. Youdim, K.[^]F. Tipton, J. Marco-Contelles, *Front Neurosci* **2016**, *10*, 205</jnl>; <lit_c><jnl>H. Wang, H. Zhang, *ACS Chem. Neurosci.* **2019**, *10*, 852--862</jnl>.
- <lit12><jnl>Z. Luo, J. Sheng, Y. Sun, C. Lu, J. Yan, A. Liu, H.[^]B. Luo, L. Huang, X. Li, *J. Med. Chem.* **2013**, *56*, 9089--9099</jnl>.
- <lit13><jnl>J. Cheung, M.[^]J. Rudolph, F. Burshteyn, M.[^]S. Cassidy, E.[^]N. Gary, J. Love, M.[^]C. Franklin, J.[^]J. Height, *J. Med. Chem.* **2012**, *55*, 10282--10286</jnl>.
- <lit14><jnl>E. Nepovimova, E. Uliassi, J. Korabecny, L.[^]E. Peña-Altamira, S. Samez, A. Pesaresi, G.[^]E. Garcia, M. Bartolini, V. Andrisano, C. Bergamini, R. Fato, D. Lamba, M. Roberti, K. Kuca, B. Monti, M.[^]L. Bolognesi, *J. Med. Chem.* **2014**, *57*, 8576--8589</jnl>.

- <lit15><lit_a><jnl>C.^J. Chou, E.^S. Inks, B.^J. Josey, *Future Med. Chem.* **2013**, 5, 857--860</jnl>; <lit_b><jnl>N. Neo^Shin, H. Jeon, Y. Jung, S. Baek, S. Lee, H.^C. Yoo, G.^H. Bae, K. Park, S.^H. Yang, J.^M. Han, I. Kim, Y. Kim, *ACS Chem. Neurosci.* **2019**, 10, 3031--3044</jnl>.
- <lit16><jnl>R. Scherzer-Attali, R. Pellarin, M. Convertino, A. Frydman-Marom, N. Egoz-Matia, S. Peled, M. Levy-Sakin, D.^E. Shalev, A. Caflisch, E. Gazit, D. Segal, *PLoS One* **2010**, 5, e11101</jnl>.
- <lit17><jnl>Y. Suhara, Y. Hirota, N. Hanada, S. Nishina, S. Eguchi, R. Sakane, K. Nakagawa, A. Wada, K. Takahashi, H. Tokiwa, T. Okano, *J. Med. Chem.* **2015**, 58, 7088--7092</jnl>.
- <lit18><jnl>A. Więckowska, K. Więckowski, M. Bajda, B. Brus, K. Sałat, P. Czerwińska, S. Gobec, B. Filipek, B. Malawska, *Bioorg. Med. Chem.* **2015**, 23, 2445--2457</jnl>.
- <lit19><lit_a><jnl>Q. Li, S. He, Y. Chen, F. Feng, W. Qu, H. Sun, *Eur. J. Med. Chem.* **2018**, 158, 463--477</jnl>; <lit_b><jnl>E. Mezeiova, K. Spilovska, E. Nepovimova, L. Gorecki, O. Soukup, R. Dolezal, D. Malinak, J. Janockova, D. Jun, K. Kuca, J. Korabecny, *J. Enzyme Inhib. Med. Chem.* **2018**, 33, 583--606</jnl>.
- <lit20><jnl>M.^L. Bolognesi, *ACS Med. Chem. Lett.* **2019**, 10, 273--275</jnl>.
- <lit21><jnl>R. Morphy, Z. Rankovic, *J. Med. Chem.* **2006**, 49, 4961--4970</jnl>.
- <lit22><jnl>J. Jeřábek, E. Uliassi, L. Guidotti, J. Korábečný, O. Soukup, V. Sepsova, M. Hrabínova, K. Kuča, M. Bartolini, L.^E. Peña-Altamira, S. Petralla, B. Monti, M. Roberti, M.^L. Bolognesi, *Eur. J. Med. Chem.* **2017**, 127, 250--262</jnl>.
- <lit23><other>M. Miyamoto, Ohta, Hiroyuki, G. Goto, Takeda Chemical Industries, Japan, **2014**</other>.
- <lit24><jnl>C. Albertini, A. Salerno, P. de^Sena^Murteira^Pinheiro, M.^L. Bolognesi, *Med. Res. Rev.* **2020**, 1--28. <https://doi.org/10.1002/med.21699>. any news?<?><?></jnl>.

- <lit25><jnl>C.[^]F.[^]J. Franco, A.[^]K. Jordão, V.[^]F. Ferreira, A.[^]C. Pinto, M.[^]C.[^]B.[^]V. de[^]Souza, J.[^]A.[^]L.[^]C. Resende, A.[^]C. Cunha, *J. Braz. Chem. Soc.* **2011**, 22, 187--193</jnl>.
- <lit26><jnl>R.[^]C. Montenegro, A.[^]J. Araújo, M.[^]T. Molina, J.[^]D. Marinho[^]Filho, D.[^]D. Rocha, E. López-Montero, M.[^]O. Goulart, E.[^]S. Bento, A.[^]P. Alves, C. Pessoa, M.[^]O. de[^]Moraes, L.[^]V. Costa-Lotufo, *Chem.-Biol. Interact.* **2010**, 184, 439--448</jnl>.
- <lit27><jnl>U. Sharma, D. Katoch, S. Sood, N. Kumar, B. Singh, A. Thakur, A. Gulati, *Indian J. Chem.* **2013**, 52B, 1431--1440</jnl>.
- <lit28><other>H. Cho (Industry-Academic Cooperation Foundation), KR 2014105413, **2014**</other>.
- <lit29><jnl>N. Jacobsen, *Org. Synth.* **2003**, 56, 68--68</jnl>.
- <lit30><jnl>L. Salmon-Chemin, E. Buisine, V. Yardley, S. Kohler, M.[^]A. Debreu, V. Landry, C. Sergheraert, S.[^]L. Croft, R.[^]L. Krauth-Siegel, E. Davioud-Charvet, *J. Med. Chem.* **2001**, 44, 548--565</jnl>.
- <lit31><jnl>G.[^]L. Ellman, K.[^]D. Courtney, V. Andres[^]Jr., R.[^]M. Featherstone, *Biochem. Pharmacol.* **1961**, 7, 88--95</jnl>.
- <lit32><jnl>A. Nordberg, C. Ballard, R. Bullock, T. Darreh-Shori, M. Somogyi, *Prim Care Companion CNS Disord* **2013**, 15, PCC.12r01412</jnl>. <?><?><?>Please abbreviated this journal!!! Thank you<?><?><?>
- <lit33><jnl>N.[^]H. Greig, D.[^]K. Lahiri, K. Sambamurti, *Int. Psychiatry Clin.* **2002**, 14 Suppl 1, 77--91</jnl>.
- <lit34><jnl>F. Prati, C. Bergamini, R. Fato, O. Soukup, J. Korabecny, V. Andrisano, M. Bartolini, M.[^]L. Bolognesi, *ChemMedChem* **2016**, 11, 1--13</jnl>.
- <lit35><jnl>E. Uliassi, L.[^]E. Peña-Altamira, A.[^]V. Morales, F. Massenzio, S. Petralla, M. Rossi, M. Roberti, L. Martinez[^]Gonzalez, A. Martinez, B. Monti, M.[^]L. Bolognesi, *ACS Chem. Neurosci.* **2019**, 10, 279--294</jnl>.

<lit36><lit_a><jnl>L. Wang, G. Esteban, M. Ojima, O.[^]M. Bautista-Aguilera, T. Inokuchi, I. Moraleda, I. Iriepa, A. Samadi, M.[^]B. Youdim, A. Romero, E. Soriano, R. Herrero, A.[^]P. Fernández, R. Fernández, R. Martínez-Murillo, J. Marco-Contelles, M. Unzeta, *Eur. J. Med. Chem.* **2014**, *80*, 543--561</jnl>; <?><?>Dear author check this journal!!<?><?> <lit_b><jnl>T.[^]P.[^]C. Chierrito, S. Pedersoli-Mantoani, C. Roca, C. Requena, V. Sebastian-Perez, W.[^]O. Castillo, N.[^]C.[^]S. Moreira, C. Pérez, E.[^]T. Sakamoto-Hojo, C.[^]S. Takahashi, J. Jiménez-Barbero, F.[^]J. Cañada, N.[^]E. Campillo, A. Martinez, I. Carvalho, *Eur. J. Med. Chem.* **2017**, *139*, 773--791</jnl>.

<lit37><jnl>J.[^]L. Cummings, T. Morstorf, K. Zhong, *Alz Res Therapy* **2014**, *6*, 1--7</jnl>.

<lit38><jnl>L. Pisani, R. Farina, M. Catto, R.[^]M. Iacobazzi, O. Nicolotti, S. Cellamare, G.[^]F. Mangiatordi, N. Denora, R. Soto-Otero, L. Siragusa, C.[^]D. Altomare, A. Carotti, *J. Med. Chem.* **2016**, *59*, 6791--6806</jnl>.

<lit39><jnl>C. Behl, B. Moosmann, *Free Radical Biol. Med.* **2002**, *33*, 182--191</jnl>.

<lit40><jnl>K.[^]S. SantaCruz, E. Yazlovitskaya, J. Collins, J. Johnson, C. DeCarli, *Neurobiol. Aging* **2004**, *25*, 63--69</jnl>.

<lit41><jnl>S. Brahmachari, A. Paul, D. Segal, E. Gazit, *Future Med. Chem.* **2017**, *9*, 797--810</jnl>.

<lit42><jnl>M. Bartolini, C. Bertucci, M.[^]L. Bolognesi, A. Cavalli, C. Melchiorre, V. Andrisano, *ChemBioChem* **2007**, *8*, 2152--2161</jnl>.

<lit43><jnl>H. Naiki, K. Higuchi, K. Nakakuki, T. Takeda, *Lab. Invest.* **1991**, *65*, 104--110</jnl>.

<lit44><book>K. Präbst, H. Engelhardt, S. Ringgeler, H. Hübner, in *Cell viability assays*, Springer, **2017**, pp. 1--17</book>.

<lit45><lit_a><jnl>L. Di, E.[^]H. Kerns, K. Fan, O.[^]J. McConnell, G.[^]T. Carter, *Eur. J. Med. Chem.* **2003**, *38*, 223--232</jnl>; <lit_b><jnl>O. Benek, O. Soukup, M. Pasdiorova, L. Hroch, V. Sepsova, P. Jost, M. Hrabínova, D. Jun, K. Kuca, D. Zala, R.[^]R. Ramsay, J. Marco-Contelles, K. Musilek, *ChemMedChem* **2016**, *11*, 1264--1269</jnl>.

<lit46><lit_a><jnl>K. Sugano, H. Hamada, M. Machida, H. Ushio, *J. Biomol. Screening*
2001, 6, 189--196</jnl>; <lit_b><jnl>F. Wohnsland, B. Faller, *J. Med. Chem.* **2001**, 44,
 923--930</jnl>.

Table¹ Inhibitory activity toward hAChE and hBuChE by compounds **5--17** and donepezil (**1**).<W=3>

Compound	<forr1>					IC ₅₀ [μM] ^[b]		SI for
	R ¹	R ²	R ³	R ⁴	X	hAChE ^[a]	hBuChE ^[a]	hAChE ^[c] 1
5	H	H	H	H	NH	22.6±1.6	14.3±0.9	0.63
6	H	H	H	OCH 3	NH	2.17±0.28	142±6	65.4
7	H	H	OCH 3	H	NH	1.53±0.29	664±405	434
8	H	H	H	OH	NH	n.a.	0.216±0.043	<0.002
9	H	CH 3	H	H	NH	47.5±11.9	0.0957±0.009 7	0.002
10	H	Cl	H	H	NH	8.03±0.54	2.48±0.04	0.31
11	OCH 3	H	H	H	NH	207±29	n.a.	-
12	OCH 3	H	H	OCH 3	NH	140±18	7.98±2.61	0.06
13	OCH 3	H	OCH 3	H	NH	115±10	93.2±17.7	0.81
14	OCH 3	H	H	OH	NH	≥75 ^[c]	n.a.	-
15	OCH 3	CH 3	H	H	NH	n.a.	0.795±0.054	<0.008

16	OCH 3	Cl	H	H	NH	n.a.	n.a.	-
17	H	CH 3	H	H	CH 2	7.84±0.28	28.2±5.9	3.60
1						0.023±0.005 ^[34]	7.42±0.39 ^[34]	323

[a] Human recombinant AChE and BuChE from human serum were used. [b] Inhibitor concentration required to decrease enzyme activity by 50%±SEM=standard error of the mean. [c] Inhibition %=20.2±1.4 at 75 μM; n.a.=not active (inhibition %<15 at 100 μM). [c] Selectivity for hAChE is determined as ratio hBuChE IC₅₀/hAChE IC₅₀.

Table 2 Prediction of BBB penetration of 7--9, 15 and reference drugs.

Compound	P_e [$10^{<M->6 \text{ cm}^s<M->1}$] ^[a]	Prediction ^[b]
7	25.73±2.01	CNS +
8	19.13±3.04	CNS +
9	6.57±0.52	CNS +
15	7.57±0.92	CNS +
donepezil (1)	21.93±2.06	CNS +
furosemide	0.19±0.07	CNS <M->
chlorothiazide	1.15±0.54	CNS <M->
ranitidine	0.35±0.31	CNS <M->
tacrine	5.96±0.59	CNS +
rivastigmine	20.00±2.07	CNS +

[a] Values are the mean±SEM ($n=3$). [b] CNS (+): high BBB permeability predicted; P_e ($10^{<M->6 \text{ cm}^s<M->1}$)>4.0. CNS (<M->): low BBB permeability predicted, P_e ($10^{<M->6 \text{ cm}^s<M->1}$)<2.0.

Scheme 1 Synthesis of compounds 5--16. a) MeCN, Na₂CO₃, 70 °C, 2 h; b) MeOH, NaBH₃CN, CH₃COONH₄, reflux, 2 h; c) DMF, MeOH or EtOH, RT, 1--4 h.

Scheme² Synthesis of compound 17. d) MeCN/H₂O (2¹), menadione (22), AgNO₃, (NH₄)₂S₂O₈, 1^h, dropwise, 65^{°C}, 2^h; e) CHCl₃, TFA, RT, 5^h; f) dry MeOH, KOH (0.17^{equiv}, pH^{4/5}), benzaldehyde, reflux, 15^{min}, NaBH₃CN, RT, 5^h.

Figure¹ Currently available AD medicines.

Figure² Rational design of novel 1-based MTDLs with expected anti-cholinesterase, anti-amyloid and antioxidant activities, inspired by our previous work.^[14]

Figure³ Cell viability determined by MTT assay. Human hepatocarcinoma cells (Hep-G2) were treated with 7, 8, 9, 15 for 24^h at a concentration ranging from 0.6 to 10^{μM}, or vehicle (DMSO). Data are presented as a percentage of viable cells in comparison with vehicle-treated controls (CTRL). Error bars indicate ±SD, *n*=3.

Figure⁴ Cell viability determined by MTT assay. Human neuroblastoma cells (SH-SY5Y) were treated with 7, 8, 9, 15 for 24^h at a concentration ranging from 0.6 to 10^{μM}, or vehicle (DMSO). Data are presented as a percentage of viable cells in comparison with vehicle-treated controls (CTRL). Error bars indicate ±SD, *n*=3.

Figure⁵ Antioxidant properties evaluation of 7, 9, 15 at 10^{μM} in comparison with vehicle (CTRL) in SH-SY5Y cells. Data are presented as percentages of DCF signal normalized to control. Error bars indicate ±SD. *[^]*P*<0.05, **[^]*P*<0.01, ***[^]*P*<0.001, ****[^]*P*<0.0001.

Figure⁶ Antioxidant properties evaluation of 7, 9, 15 at 10^{μM} in comparison with vehicle (CTRL). Oxidative stress was induced by treating SH-SY5Y cells with 100^{μM} TBH for 30^{min}. Data are presented as percentages of DCF signal normalized to control. Error bars indicate ±SD. *[^]*P*<0.05, **[^]*P*<0.01, ***[^]*P*<0.001, ****[^]*P*<0.0001.

Figure⁷ Antioxidant properties evaluation of 7, 9, 15 at 10^{μM} in comparison with vehicle (CTRL) after an oxidative stress induction by pre-treating SH-SY5Y cells with 2.5^{μM} sulforaphane (S). Data are presented as percentage of DCF signal normalized to control. Error bars indicate ±SD. *[^]*P*<0.05, **[^]*P*<0.01, ***[^]*P*<0.001, ****[^]*P*<0.0001.

Figure⁸ Antioxidant properties evaluation of 7, 9, 15 at 10^{μM} in comparison with vehicle (CTRL). Oxidative stress was induced by exposing SH-SY5Y cells, pre-treated for 24^h with 2.5^{μM} sulforaphane (S), to 100^{μM} TBH for 30^{min}. Data are presented as percentages of DCF signal normalized to control. Error bars indicate ±SD. *[^]*P*<0.05, **[^]*P*<0.01, ***[^]*P*<0.001, ****[^]*P*<0.0001.

Figure⁹ Cell viability determined by MTT assay. Primary rat cerebellar granule neurons (CGNs) were treated with 9 for 24^h at a concentration ranging from 1^{μM} to

50^μM in comparison with control. Data are presented as a percentage of viable cells in comparison with vehicle-treated controls. Error bars indicate ±ES of two different experiments each run in quadruplicate. *^P<0.05, **^P<0.01, compared to control conditions (0^μM) Dunnett's test after ANOVA.